

## Restenosis after balloon valvuloplasty in a dog with pulmonary stenosis

Hiroshi SUNAHARA<sup>1</sup>), Yoko FUJII<sup>1</sup>)\*, Keisuke SUGIMOTO<sup>1</sup>), Takuma AOKI<sup>1</sup>), Gou SUGAHARA<sup>2</sup>) and Kinji SHIROTA<sup>2</sup>)

<sup>1</sup>Laboratory of Surgery 1, Azabu University, 1-17-71 Fuchinobe, Chuo-ku, Sagamihara-shi, Kanagawa 252-5201, Japan

<sup>2</sup>Laboratory of Veterinary Pathology, Azabu University, 1-17-71 Fuchinobe, Chuo-ku, Sagamihara-shi, Kanagawa 252-5201, Japan

(Received 10 May 2014/Accepted 3 September 2014/Published online in J-STAGE 23 September 2014)

**ABSTRACT.** A two-month-old female Chihuahua was diagnosed as severe pulmonary valvular stenosis (PS). Although balloon valvuloplasty (BV) was successfully performed, restenosis was observed 19 months after the procedure. Euthanasia was chosen due to low output syndrome during the surgical repair attempted when the dog was 5 years old. Postmortem examination revealed markedly thickened pulmonary valve due to the increase of extracellular matrix which might be produced by increased  $\alpha$  smooth muscle actin-positive myofibroblasts. The thickening of the valve was associated with restriction of the valve's motion, resulting in restenosis in the present case. This is the first case report documented histopathological and immunohistochemical findings of the restenotic pulmonary valve in dogs with PS after BV.

**KEY WORDS:** canine, pulmonary stenosis, restenosis

doi: 10.1292/jvms.14-0242; *J. Vet. Med. Sci.* 77(1): 95–99, 2015

Balloon valvuloplasty (BV) has become the first-line treatment for dogs with moderate to severe pulmonary valvular stenosis (PS) [11]. A previous study demonstrated that BV improved clinical signs and survival time [1], and BV has been recognized as an effective and safe technique in humans and dogs when performed in indicated patients [3, 7, 19].

Complications in long-term follow-up, such as residual pressure gradient, pulmonary valve regurgitation and restenosis, were reported in a human study with over 10 years of follow-up [20]. Frequency of restenosis in several human case series ranged from 4.8–21% [19], but reports of long-term outcomes after BV have been limited in veterinary medicine. Small case series with 1–6 months follow-up after BV reported that restenosis was observed in some dogs, although the details were not discussed [7]. The cause of restenosis in dogs has never been described, and no study has documented histopathological and immunohistochemical findings of the restenotic pulmonary valve in dogs with PS after BV.

A 2-month-old female Chihuahua, weighing 660 g, was referred to Azabu University Veterinary Teaching Hospital, because of a cardiac murmur (day 1). The dog was asymptomatic, and physical examination was unremarkable except for a grade 5/6 systolic ejection murmur at the left heart base and systolic regurgitant murmur at the right heart apex. Thoracic radiography revealed right ventricular and main pulmonary arterial enlargement. Normal sinus rhythm with right mean electrical axis deviation was observed on an elec-

trocardiogram. Echocardiography revealed right ventricular hypertrophy and dilation, flattening of the interventricular septum, perimembranous ventricular septal defect (VSD) with left-to-right shunt and severe pulmonary stenosis. Ventricular septal defect was considered as relatively small on B-mode and Color-Doppler images. Pulmonary annulus diameter was 9 mm, the same as the aortic diameter. Pulmonary valve commissures were fused with a central orifice, and valve doming in systole was observed (valvular stenosis). The peak instantaneous pressure gradient across the pulmonary valve was estimated to be 92 mmHg (maximal pulmonary arterial blood flow velocity, 4.8 m/s). Since the peak VSD flow was 2.2 m/s, the estimated pressure gradient between left and right ventricles was 19 mmHg. No volume overload in left side of the heart was observed. The dog was diagnosed as severe pulmonic valvular stenosis with restricted VSD. Since PS was considered to be the major

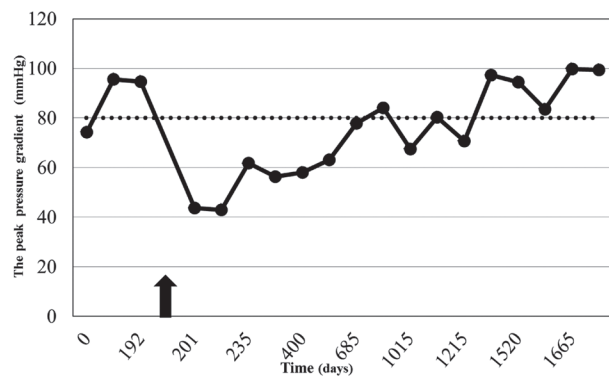


Fig. 1. The peak instantaneous pressure gradient across the pulmonary valve (mmHg) estimated by Doppler echocardiography from day 1 to 1714. BV was performed on day 200 (arrow). The peak pressure gradient was consistently increased over time and exceeded 80 mmHg (dotted line) on day 768.

\*CORRESPONDENCE TO: FUJII, Y., Azabu University, 1-17-71 Fuchinobe, Chuo-ku, Sagamihara-shi, Kanagawa 252-5201, Japan.  
e-mail: fujiiy@azabu-u.ac.jp

©2015 The Japanese Society of Veterinary Science

This is an open-access article distributed under the terms of the Creative Commons Attribution Non-Commercial No Derivatives (by-nc-nd) License <http://creativecommons.org/licenses/by-nc-nd/3.0/>.

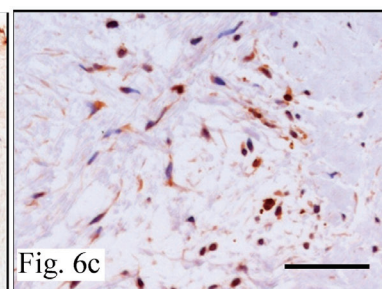
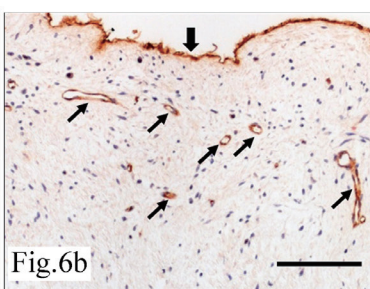
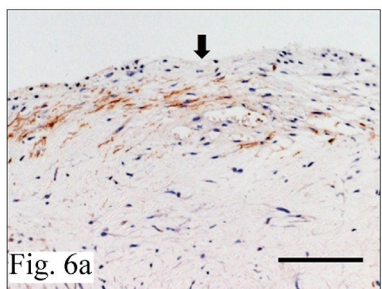
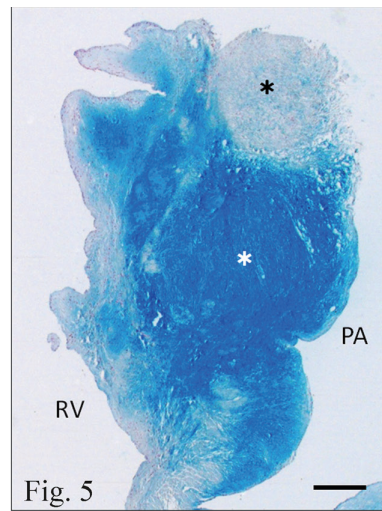
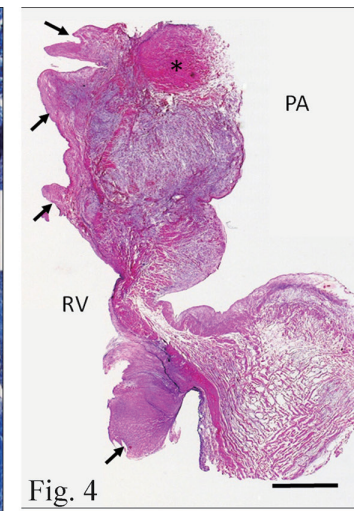
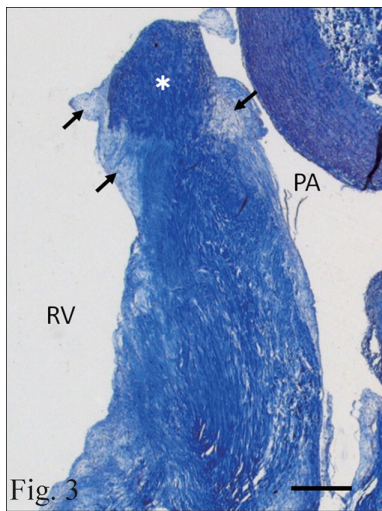
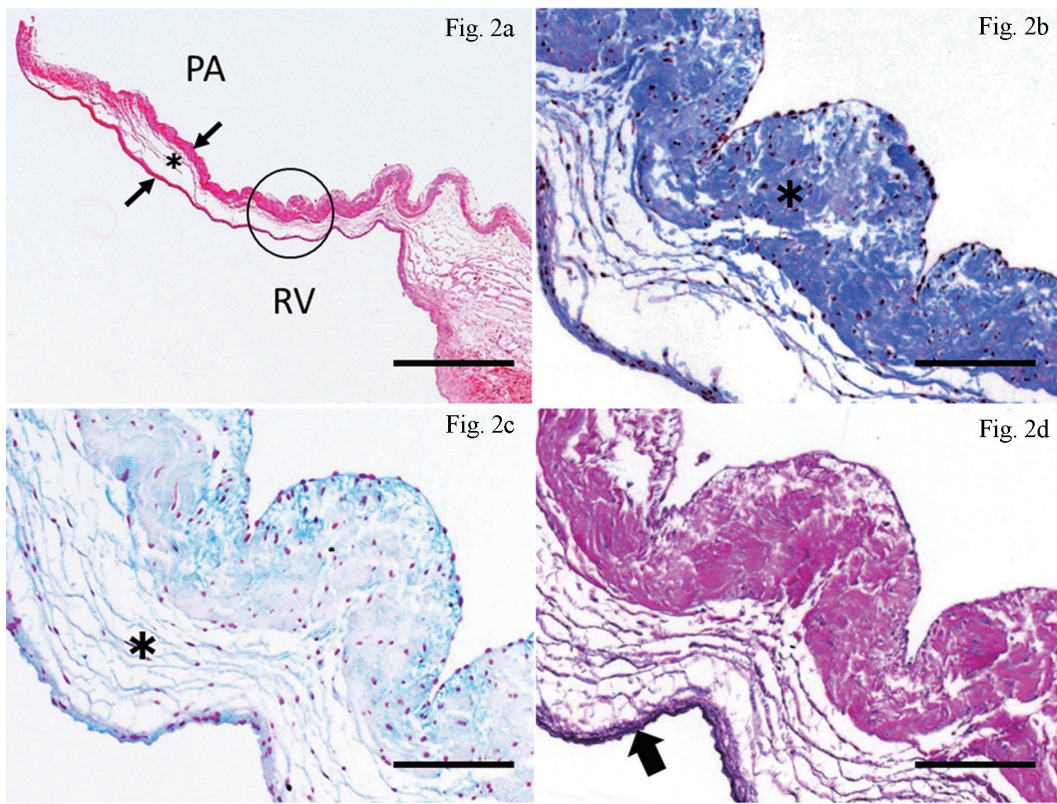


Table 1. Primary antibodies and immunostaining protocol

Antibody <sup>a)</sup>	Clone	Dilution	Source <sup>b)</sup>	Target	Antigen retrieval <sup>c)</sup>
Iba-1		1:100	Wako	macrophages	MW, 99°C, 20 min
vWF		prediluted	DAKO	vascular endothelial cells	Pepsin, 37°C, 20 min
SMA	1A4	1:50	DAKO	vascular smooth muscle cells, pericytes, myofibroblasts	NT
PCNA	PC10	1:100	DAKO	proliferating cells	MW, 90°C, 10 min
CD3		1:400	DAKO	T lymphocytes	Pepsin, 37°C, 20 min
CD20		1:400	Thermo Fisher Scientific	B lymphocytes	NT
Fibrinogen		1:1000	DAKO	Fibrinogen, fibrin	Trypsin, 37°C, 30 min

a) vWF= von Willebrand factor; SMA= $\alpha$ -smooth muscle actin; PCNA=proliferating cell nuclear antigen; NT=no treatment. b) Wako Pure Chemical Industries Ltd., Osaka, Japan; Dako Denmark A/S, Glostrup, Denmark; Thermo Fisher Scientific (Anatomic Pathology), Fremont, CA, U.S.A. c) MW=microwave, citrate buffer (PH6.0); Pepsin=0.4%Pepsin (Dako); Trypsin=0.1% trypsin (Dako).

lesion in this particular case, BV was performed on day 200.

Following intravenous administration of fentanyl (10  $\mu$ g/kg, Fentanyl, Janssen Pharmaceutical, Tokyo, Japan) and midazolam (0.2 mg/kg, Dormicum, Astellas Pharma, Tokyo, Japan), general anesthesia was maintained by isoflurane (Isoflurane, Canonsburg, PA, U.S.A.) and fentanyl (continuous rate infusions 10  $\mu$ g/kg/hr). Cardiac catheterization (Multipurpose catheter, Medikit Co., Tokyo, Japan) was performed through right external jugular vein. Systolic pressure in right ventricle and main pulmonary artery were 72 and 10 mmHg, respectively. Selective right ventricular angiography revealed PS with poststenotic dilatation. Since the pulmonary valve annulus diameter was 8.5 mm, BV was performed using a balloon (TYSHAK IIVeterinary Balloon Catheter, NuMed, Hopkinton, NY, U.S.A.) size of 12 mm (1.4 times the width of annulus). The balloon was inflated twice until the waist disappeared. The peak right ventricular pressure was decreased to 28 mmHg. The dog recovered uneventfully from the anesthesia.

On day 208 (a week after the procedure), echocardiographic examination using right parasternal short-axis view revealed that the peak instantaneous pressure gradient across

the pulmonary valve decreased to 43 mmHg (maximal pulmonary arterial blood flow velocity, 3.3 m/s). Although the peak VSD flow increased to 4.7 m/s, left atrial-to-aortic root diameter ratio, left ventricular diameter at the end-diastole (1.53 cm, 95% prediction interval; 1.67–2.43 cm) and left ventricular end-diastolic diameter index (1.17) were within normal range, which revealed that there was no deterioration of volume overload to the left heart. Follow-up echocardiography was performed every 1–3 months (Fig. 1). On day 685, the pressure gradient across the pulmonary valve increased to 78 mmHg, and because the pressure gradient was consistently increased over 80 mmHg after day 768, atenolol was prescribed. Because exacerbation of stenosis was observed and the dog started showing exercise intolerance, surgical repair under the cardiopulmonary bypass was performed on day 1,717. The right ventricular outflow tract and pulmonary artery were dissected, and the stenotic pulmonary cusp was excised. The dog developed low output syndrome after weaning from artificial cardiopulmonary support. Since the response to medical assistance was poor, euthanasia was chosen.

After euthanasia, the heart was removed and immediately

Fig. 2. Histological feature of a normal cusp of the pulmonary valve from control beagle dog. (a) Upper and lower arrows indicate the fibrosa and ventricularis of a cusp, respectively. Asterisk showed spongiosa, which had artificially distended during tissue processing. Hematoxylin and eosin staining. (b) Fibrosa (\*) consists of thick bundles of collagen fibers. Masson's trichrome. (c) Spongiosa (\*) consists of fine collagen fibers, scattered mesenchymal cells and alcian blue (AB) positive matrix. Alcian blue. (d) Ventricularis is composed of densely arranged elastic fibers (arrow). Elastica van Gieson. Figures (b), (c) and (d) are of the area encircled in (a). PA: pulmonary artery aspect. RV: right ventricular aspect. Bar=800  $\mu$ m (a) and 200  $\mu$ m (b, c, d).

Fig. 3. The left-facing cusp of the case, showing severe fibrosis. The cusp was replaced by dense collagen fibers seen in deep blue. The tip of the cusp (\*) composed of dense collagen fibers as well as elastic fibers. Some lucent portions protruded from the surface of the cusp (arrows). PA: pulmonary artery aspect. RV: right ventricular aspect. Masson's trichrome. Bar=400  $\mu$ m.

Fig. 4. The non-facing cusp of the case, showing lumpy configuration. Irregular protrusions of the valvular tissue developed from the ventricular surface of the cusp (arrows). Asterisk indicates nodule of semilunar valve. PA: pulmonary artery aspect. RV: right ventricular aspect. Elastica van Gieson. Bar=800  $\mu$ m.

Fig. 5. Massive deposition of Alcian blue-positive matrix in the non-facing cusp of the case (white asterisk) as shown in Fig. 4. Nodule of semilunar valve was faintly stained (black asterisk). PA: pulmonary artery aspect. RV: right ventricular aspect. Alcian blue. Bar=400  $\mu$ m.

Fig. 6. Immunohistochemical findings of the non-facing cusp of the case. (a) Elongated  $\alpha$ SMA-positive myofibroblasts accumulated in the valvular tissue. Arrow indicates valvular surface. (b) Development of small blood vessels, of which endothelium showed positive for von Willebrand factor (small arrows). Endothelium of valvular surface was also positive for this endothelial marker (large arrow). (c) Iba-1-positive macrophages infiltrated in the cusps. Immunostaining for  $\alpha$ SMA (a), von Willebrand factor (b) and Iba-1 (c). Positive reaction was visualized as brown in color. Bar=100  $\mu$ m (a, b) and 50  $\mu$ m (c).

immersed in 10% neutral-buffered formalin. The cusps of the pulmonary valve were excised from the heart, embedded in paraffin, sectioned at 4  $\mu\text{m}$  thickness and stained with hematoxylin and eosin, alcian blue (AB) (pH 2.5 for acid mucopolysaccharide), Masson's trichrome (MTC) and Elastic Van Gieson Stains. Immunohistochemical staining were performed on the paraffin sections using an immunoenzyme polymer method, and primary antibodies, dilutions and antigen retrieval are shown in Table 1. Peroxidase-conjugated anti-mouse immunoglobulin G (Histofine Simple Stain MAX-PO (M); Nichirei, Tokyo, Japan) or peroxidase-conjugated anti-rabbit immunoglobulin G (Histofine Simple Stain MAX-PO) ((R); Nichirei) was used as a secondary antibody. After immunoreactions, the sections were colorized with diaminobenzidine and counterstained with Mayer's hematoxylin.

The pulmonary valves from three beagles (control dogs, 12–18 months old, weighing 10.4 to 11.2 kg) without any cardiac abnormalities were examined by the same methods for comparison. This study was approved by the Ethical Committee of Azabu University (No.1306105) and conducted in accordance with guidelines established by the Animal Welfare Act and the NIH Guide for Care and Use of Laboratory Animals.

Macroscopically, the cusps of pulmonary valves from control dogs were thin and semilunar in shape. The size and shape of cusps were approximately the same in each control dog. On the other hand, cusps of the restenotic pulmonary valve of the present case were prominently thickened, stiff and irregular in shape. Other valves including atrioventricular valves and aortic valve from the present case were macroscopically unremarkable.

Light microscopy revealed that the cusps of the pulmonary valves in control dogs were entirely covered with a single layer of endothelial cells and composed of three distinct layers: the fibrosa (pulmonary artery aspect), the spongiosa (inner aspect) and the ventricularis (ventricular aspect), as in human heart [2] (Fig. 2a). The fibrosa was composed of bundles of collagen fibers (Fig. 2b), and the spongiosa was a thin lucent layer containing AB-positive materials, delicate collagen fibers and scattered fibroblasts (Fig. 2c). This layer was well developed at the base of the cusps. The ventricularis was thin and mainly composed of elastic fibers (Fig. 2d). A few  $\alpha$  smooth muscle actin ( $\alpha\text{SMA}$ )-positive cells were present beneath the surface endothelial cells in the ventricular aspect, and no blood vessels were found in the cusps of control dogs. Few Iba-1-positive macrophages were scattered throughout the cusps, but proliferating cells positive for proliferating nuclear antigen (PCNA) were not detected in control pulmonary valves.

In the restenotic valve of the present patient, three cusps were markedly thickened, and the three layers were no longer distinguished. The left-facing cusp showed intense fibrosis with focal deposition of the AB-positive matrix (Fig. 3). Also, while elastofibrosis and irregular protrusions developed at the tip of the cusp, the right-facing and non-facing cusps showed a lumpy configuration with massive deposition of the AB-positive matrix (Figs. 4 and 5).

Characteristic irregular protrusions of valvular tissue were developed on the ventricular surface of these cusps. Multifocal proliferation of  $\alpha\text{SMA}$ -positive myofibroblasts (Fig. 6a) and development of small blood vessels confirmed by immunostaining for von Willebrand factor (Fig. 6b) were detected in these affected valvular tissues, particularly in the ventricular aspect. PCNA-positive spindle cells and Iba-1 positive macrophages (Fig. 6c) were increased in number and diffusely distributed in the cusps. Except for deposition of the AB-positive matrix, vascular development, myofibroblast proliferation and irregular configuration of the valvular surface were more prominent in the ventricular aspect than in the pulmonary artery aspect of the cusps, as described.

In CD3 and CD20-positive cells, fibrinogen-positive matrix was not detected, neither in control pulmonary valves nor the restenotic valve.

Restenosis after BV in patients with PS is known to be one of the common complications in human patients [2, 16, 22]. Earlier investigators reported that inadequate balloon size and pulmonary valve dysplasia were factors that have been related to restenosis [6, 9, 14, 17, 18]. In our case, pulmonary valvular annulus did not show narrowing or hypodysplasia (Type A, according to Bussadori *et al.* [3]), which was indicated for BV. The recommended balloon size on the basis of pulmonary annulus diameter was 10 mm to 12 mm in this case, so we chose an adequate balloon size (12 mm) [1, 4, 5, 21].

The affected valve was markedly thickened due to an increased amount of the AB-positive extracellular matrix, which was composed of acid mucopolysaccharide and collagen fibers. It was suggested that thickening of the valve due to the increase of extracellular matrix would be associated with narrowing of the valve opening, resulting in restenosis. Immunohistochemical examination revealed prominently increased  $\alpha\text{SMA}$ -positive myofibroblasts in the affected valve. These myofibroblasts are known to be active forms of fibroblasts [8] and produce acid mucopolysaccharide and collagen following tissue injury [13, 15]. Also, the increased number of Iba-positive macrophages and development of blood vessels in the affected valve suggested that an (inflammatory) organization process had taken place in the injured tissue. The activated macrophages might secrete IL-6, which activates fibroblasts [12], and could also be involved in the angiogenesis observed in the affected valve.

As described above, restenosis appeared to be associated with thickening of the valve induced by activation of myofibroblasts, possibly due to (inflammatory) organization response in the valvular injured tissue after BV. However, severity of stenosis worsened about 1.5 years post-BV in our case. This implied that stenosis would not be caused by an acute inflammatory response due to injury from the balloon procedure. Leslie *et al.* reported that mechanical stress was partly responsible for the changes in connective tissue that occur as a result of pressure overload [10]. Although the severity was mild to moderate, residual stenosis was observed immediately after BV in our patient. Mechanical stress might have partly contributed to remodeling of the pulmonary valve. Vascular formation and accumulation

of myofibroblasts were more prominent in the ventricular aspect of the cusps, indicating a tissue response to the mechanical stress on the cusps.

Further studies are warranted to confirm our hypothesis that mechanical stress contributes to restenotic process and investigate the exact cause of restenosis after BV, and to develop possible treatment options to prevent restenosis.

## REFERENCES

- Berman, W. Jr., Fripp, R. R., Raisher, B. D. and Yabek, S. M. 1999. Significant pulmonary valve incompetence following oversize balloon pulmonary valvuloplasty in small infants: A long-term follow-up study. *Catheter. Cardiovasc. Interv.* **48**: 61–65. [[Medline](#)] [[CrossRef](#)]
- Billingham, M. E. 1997. *Histology for Pathologists*, 2nd ed., Lippincott-Raven Publishers, New York.
- Bussadori, C., DeMadron, E., Santilli, R. A. and Borgarelli, M. 2001. Balloon valvuloplasty in 30 dogs with pulmonic stenosis: effect of valve morphology and annular size on initial and 1-year outcome. *J. Vet. Intern. Med.* **15**: 553–558. [[Medline](#)] [[Cross-Ref](#)]
- Estrada, A., Moïse, N. S., Erb, H. N., McDonough, S. P. and Renaud-Farrell, S. 2006. Prospective evaluation of the balloon-to-annulus ratio for valvuloplasty in the treatment of pulmonic stenosis in the dog. *J. Vet. Intern. Med.* **20**: 862–872. [[Medline](#)] [[CrossRef](#)]
- Harrild, D. M., Powell, A. J., Tran, T. X., Geva, T., Lock, J. E., Rhodes, J. and McElhinney, D. B. 2010. Long-term pulmonary regurgitation following balloon valvuloplasty for pulmonary stenosis risk factors and relationship to exercise capacity and ventricular volume and function. *J. Am. Coll. Cardiol.* **55**: 1041–1047. [[Medline](#)] [[CrossRef](#)]
- Jeffery, R. F., Moller, J. H. and Amplatz, K. 1972. The dysplastic pulmonary valve: a new roentgenographic entity; with a discussion of the anatomy and radiology of other types of valvular pulmonary stenosis. *Am. J. Roentgenol. Radium Ther. Nucl. Med.* **114**: 322–339. [[Medline](#)] [[CrossRef](#)]
- Johnson, M. S. and Martin, M. 2004. Results of balloon valvuloplasty in 40 dogs with pulmonic stenosis. *J. Small Anim. Pract.* **45**: 148–153. [[Medline](#)] [[CrossRef](#)]
- Junqueira, L. C. and Carneiro, J. 2003. *Basic Histology, Text & Atlas*, 10th ed., McGraw-Hill Medical, New York.
- Koretzky, E. D., Moller, J. H., Korn, M. E., Schwartz, C. J. and Edwards, J. E. 1969. Congenital pulmonary stenosis resulting from dysplasia of valve. *Circulation* **40**: 43–53. [[Medline](#)] [[CrossRef](#)]
- Leslie, K. O., Taatjes, D. J., Schwarz, J., vonTurkovich, M. and Low, R. B. 1991. Cardiac myofibroblasts express alpha smooth muscle actin during right ventricular pressure overload in the rabbit. *Am. J. Pathol.* **139**: 207–216. [[Medline](#)]
- Locatelli, C., Spalla, I., Domenech, O., Sala, E., Brambilla, P. G. and Bussadori, C. 2013. Pulmonic stenosis in dogs: survival and risk factors in a retrospective cohort of patients. *J. Small Anim. Pract.* **54**: 445–452. [[Medline](#)] [[CrossRef](#)]
- Ma, F., Li, Y., Jia, L., Han, Y., Cheng, J., Li, H., Qi, Y. and Du, J. 2012. Macrophage-stimulated cardiac fibroblast production of IL-6 is essential for TGF  $\beta$ /Smad activation and cardiac fibrosis induced by angiotensin II. *PLoS ONE* **7**: e35144. [[Medline](#)] [[CrossRef](#)]
- Milara, J., Serrano, A., Peiró, T., Gavalda, A., Miralpeix, M., Morcillo, E. J. and Cortijo, J. 2012. Acridinium inhibits human lung fibroblast to myofibroblast transition. *Thorax* **67**: 229–237. [[Medline](#)] [[CrossRef](#)]
- Musewe, N. N., Robertson, M. A., Benson, L. N., Smallhorn, J. F., Burrows, P. E., Freedom, R. M., Moes, C. A. and Rowe, R. D. 1987. The dysplastic pulmonary valve: echocardiographic features and results of balloon dilatation. *Br. Heart J.* **57**: 364–370. [[Medline](#)] [[CrossRef](#)]
- Ohkawa, T., Ueki, N., Taguchi, T., Shindo, Y., Adachi, M., Amuro, Y., Hada, T. and Higashino, K. 1999. Stimulation of hyaluronan synthesis by tumor necrosis factor-alpha is mediated by the p50/p65 NF-kappa B complex in MRC-5 myofibroblasts. *Biochim. Biophys. Acta* **1448**: 416–424. [[Medline](#)] [[CrossRef](#)]
- Peterson, C., Schilthuis, J. J., Dodge-Khatami, A., Hitchcock, J. F., Meijboom, E. J. and Bennink, G. B. 2003. Comparative long-term results of surgery versus balloon valvuloplasty for pulmonary valve stenosis in infants and children. *Ann. Thorac. Surg.* **76**: 1078–1082. [[Medline](#)] [[CrossRef](#)]
- Radtke, W., Keane, J. F., Fellows, K. E., Lang, P. and Lock, J. E. 1986. Percutaneous balloon valvotomy of congenital pulmonary stenosis using oversized balloons. *J. Am. Coll. Cardiol.* **8**: 909–915. [[Medline](#)] [[CrossRef](#)]
- Rao, P. S. 1987. Influence of balloon size on short-term and long-term results of balloon pulmonary valvuloplasty. *Tex. Heart Inst. J.* **14**: 57–61. [[Medline](#)]
- Rao, P. S. 2007. Percutaneous balloon pulmonary valvuloplasty: state of the art. *Catheter. Cardiovasc. Interv.* **69**: 747–763. [[Medline](#)] [[CrossRef](#)]
- Rao, P. S., Galal, O., Patnana, M., Buck, S. H. and Wilson, A. D. 1998. Results of three to 10 year follow up of balloon dilatation of the pulmonary valve. *Heart* **80**: 591–595. [[Medline](#)]
- Rao, P. S., Thapar, M. K. and Kutayli, F. 1988. Causes of restenosis after balloon valvuloplasty for valvular pulmonary stenosis. *Am. J. Cardiol.* **62**: 979–982. [[Medline](#)] [[CrossRef](#)]
- Voet, A., Rega, F., de Bruaene, A. V., Troost, E., Gewillig, M., Van Damme, S. and Budts, W. 2012. Long-term outcome after treatment of isolated pulmonary valve stenosis. *Int. J. Cardiol.* **156**: 11–15. [[Medline](#)] [[CrossRef](#)]